



ELSEVIER

Journal of Volcanology and Geothermal Research 72 (1996) 85–100

Journal of volcanology
and geothermal research

Caldera morphology in the western Galápagos and implications for volcano eruptive behavior and mechanisms of caldera formation

Duncan C. Munro^{*}, Scott K. Rowland

Hawai'i Institute of Geophysics and Planetology, School of Ocean and Earth Science and Technology, 2525 Correa Rd., Honolulu, HI 96822, USA

Received 12 October 1993; accepted 16 October 1995

Abstract

Caldera morphology on the six historically active shield volcanoes that comprise Isabela and Fernandina islands, the two westernmost islands in the Galápagos archipelago, is linked to the dynamics of magma supply to, and withdrawal from, the magma chamber beneath each volcano. Caldera size (e.g., volumes 2–9 times that of the caldera of Kilauea, Hawai'i), the absence of well-developed rift zones and the inability to sustain prolonged low-volumetric-flow-rate flank eruptions suggest that magma storage occurs predominantly within centrally located chambers (at the expense of storage within the flanks). The calderas play an important role in the formation of distinctive arcuate fissures in the central part of the volcano: repeated inward collapse of the caldera walls along with floor subsidence provide mechanisms for sustaining radially oriented least-compressive stresses that favor the formation of arcuate fissures within 1–2 km outboard of the caldera rim. Variations in caldera shape, depth-to-diameter ratio, intra-caldera bench location and the extent of talus slope development provide insight into the most recent events of caldera modification, which may be modulated by the episodic supply of magma to each volcano. A lack of correlation between the volume of the single historical collapse event and its associated volume of erupted lava precludes a model of caldera formation linked directly to magma withdrawal. Rather, caldera collapse is probably the result of accumulated loss from the central storage system without sufficient recharge and (as has been suggested for Kilauea) may be aided by the downward drag of dense cumulates and intrusives.

1. Introduction

The Galápagos archipelago is an oceanic hotspot group of at least twenty subaerial volcanoes. The

western part of the archipelago has the youngest volcanoes, nine of which have erupted since 1813, when written records were initiated. The most active volcanoes are those of Isabela and Fernandina islands (Fig. 1), and it is here that the calderas occur. These volcanoes erupt tholeiite basalt (McBirney and Williams, 1969), and appear to have grown contemporaneously.

The subaerial form of Galápagos volcanoes has been described numerous times (e.g., McBirney and Williams, 1969; Nordlie, 1973; Simkin, 1984). In

^{*} Corresponding author. Present address: Western European Union Satellite Centre, P.O. Box 511, U.E.O., SP 28850 Torrejon de Ardoz, Madrid, Spain. Tel.: +34-1-6777-759 (office hours); +34-1- 881-4765 (home). Fax: +34-1-677-7228. E-mail: 100520.2413@compuserve.com.

phology and the distribution of eruptive activity in the vicinity of the caldera to deduce the influence of caldera-related processes on the eruptive behavior of each volcano. Calderas form by subsidence associated with magma chamber complexes (e.g., Williams and McBirney, 1979). Modes of subsidence vary widely, ranging from broad down-sagging between bounding linear faults, through piston-like descent of a coherent cylinder along bounding ring faults, to the piecemeal collapse of small segments of the caldera floor producing a funnel-shaped morphology which may be significantly asymmetric with respect to the caldera center (Walker, 1988). The simplest (and oldest) model for caldera formation links subsidence directly to the evacuation of a magma chamber (e.g., Dutton, 1884), and may be applicable to some explosive rhyolite complexes. However, on basaltic volcanoes this mechanism clearly is not supported by evidence from the Hawaiian volcanoes Mauna Loa and Kilauea: (1) eruptive vents rarely occur along caldera-boundary faults; (2) eruptive volumes don't equal collapse volumes; and (3) cumulative subsidence is funnel shaped rather than piston shaped (Walker, 1988). Additionally, there is the important idea that calderas collapse and re-fill many times during the life of a basaltic volcano (Macdonald, 1965; Decker, 1987). Walker (1988) attributed subsidence of the Kilauea caldera to down-sagging due to crystal cumulates at the base of, and a "coherent intrusion complex" adjacent to, a near-surface magma chamber.

2. Methodology

In this paper, the calderas of Wolf, Darwin, Alcedo, Sierra Negra and Cerro Azul (Isla Isabela) and Fernandina (Isla Fernandina) are described utilizing SPOT HRV-1 satellite images, topographic data available from the United States Defense Mapping Agency sheets 22451–22455 and field observations made at Fernandina in 1989 (Rowland and Munro, 1992). We have also made limited use of TOPSAR interferometric radar-derived topography (e.g., Evans et al., 1992; Zebker et al., 1992; Farr et al., 1995). These data were collected in May of 1993, and provide 2–3 m vertical resolution with 10 m ground pixels.

The SPOT HRV-1 instrument in panchromatic (black and white) mode, covers the visible region of the electromagnetic spectrum in one waveband at a spatial resolution of 10 m per pixel (Chevrel et al., 1981). The major advantage of SPOT HRV-1 over previous satellite-imaging systems is that it has the capability to be pointed off-nadir, making it possible to view one area on the Earth's surface on successive overpasses and increasing the data collection opportunities in regions where cloud cover is common. This off-nadir viewing capability was a key element in obtaining complete coverage of Isabela and Fernandina islands between April 1988 and March 1989. Five images were mosaicked to eliminate overlap and the raw data were placed into a geometrically consistent Universal Transverse Mercator (UTM) Projection. From these processed images, sketch maps of structural and eruptive features were made to highlight their spatial distribution (Figs. 2–7). The images shown in Figs. 2–7 have been contrast enhanced to show the maximum detail possible. It is important to note that the illumination and viewing geometry differ for each SPOT HRV-1 image used in this study so it is not possible to directly compare the albedos of surface units from one volcano to another.

A disadvantage of the SPOT HRV-1 data is that the spatial resolution (10 m per pixel) is too low for the identification of closely spaced fissures that occur in the summit regions of the volcanoes (Chadwick and Howard, 1991). Additionally, in areas where many lava flows are juxtaposed, variations in surface albedo may be too subtle to discern all lava-flow boundaries. For these reasons our interpretations concentrate on caldera morphology and the general distribution of eruptive features on each volcano. Where possible, the boundaries of individual flows were mapped, but observations in the field and some limited air-photo examinations clearly indicate that many more flow units exist on the ground than can be distinguished in the SPOT data. Thus, the areas denoted as lava flows on the maps (Fig. 2B Fig. 3B Fig. 4B Fig. 5B Fig. 6B Fig. 7B) represent only an approximation of the distribution of recent lava flows. Despite the limitations in resolution, the SPOT data still provide many clues to the structural influences of the Galápagos calderas on volcano eruptive behavior.

3. Descriptions of Galápagos calderas

The following section presents the SPOT images, sketch maps and descriptions of features that bear on our interpretations of caldera morphology, vent orientation and vent distribution.

3.1. Volcán Wolf

The caldera of Volcán Wolf (Fig. 2) has a maximum depth of 660 m. The rim of the caldera is slightly elongated along a NW–SE trend (Table 1)

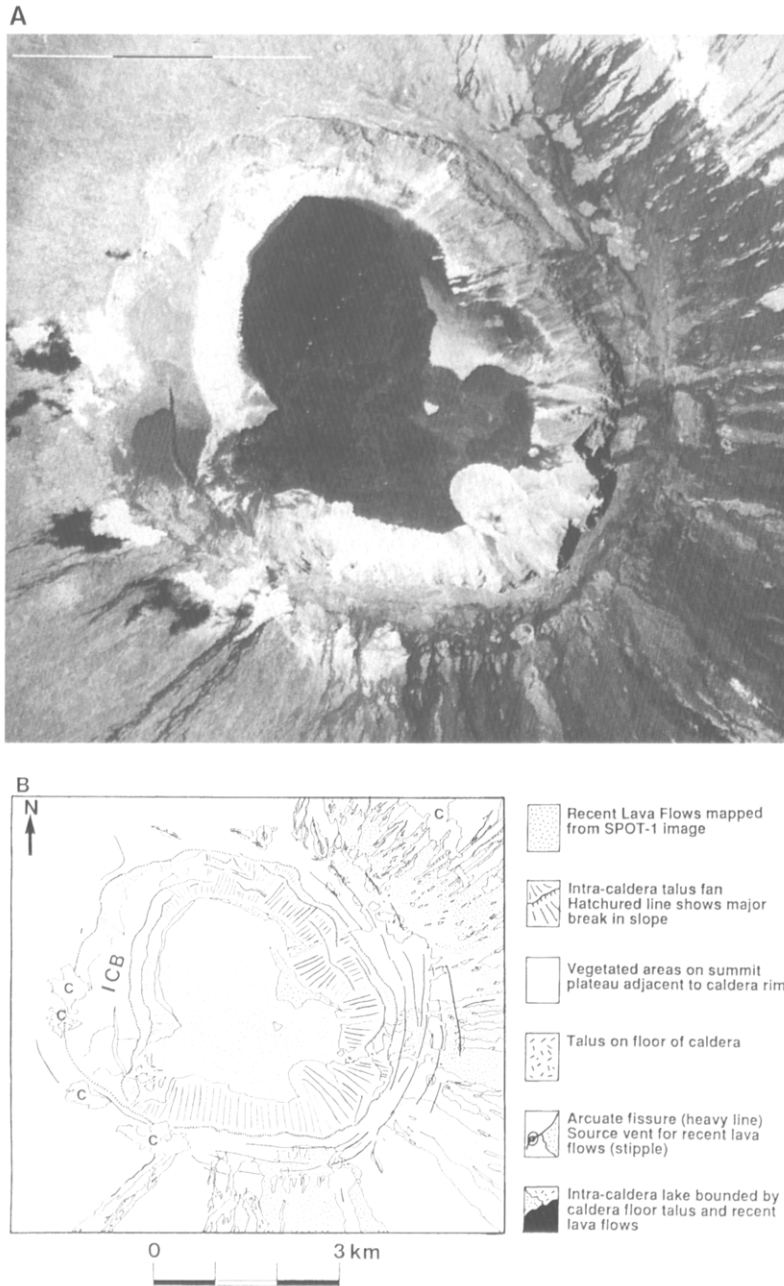


Fig. 2. The caldera of Volcán Wolf. (A) SPOT image. (B) Sketch map. C = clouds in SPOT image; ICB = intra-caldera bench.

and shows poorly defined arcuate embayments to the west above a major intra-caldera bench. Talus slopes extend from the southern rim all the way to the caldera floor. The eastern and northern walls are composed of talus slopes that are interrupted by well-defined breaks in slope. These breaks suggest that slumping of talus fans toward the caldera center occurs, destabilizing the caldera walls, and promoting continuous degradation of the caldera rim. Several lava flows that originated from vents on the eastern summit plateau drape the eastern talus slopes. A distinctive lobe of material in the southeastern corner of the caldera is interpreted to be a landslide deposit. The western segment of the caldera is dominated by a major bench, the top of which lies 120 m below the rim and 380 m above the caldera floor (measurements made from DMA Sheet # 22543). The bench has two segments separated by a broad ridge of talus that descends from the caldera rim; a smaller semi-circular segment occurs to the north, and an elongate portion extends to the south. A prominent cleft is seen in the southern portion of the bench and lava from a vent located to the west has flowed across the bench into the cleft and thence onto the caldera floor. The caldera floor is elongated along a similar NW–SE trend to the rim and is covered by pahoehoe lava that issued from vents beneath the southwestern wall during an eruption in 1982 (McLelland et al., 1989). The pattern of bench

and talus development within the caldera suggests that subsidence is at a maximum in the south and at a minimum in the west.

3.2. Volcán Darwin

The caldera of Volcán Darwin (Fig. 3) is approximately 200 m deep. There are no major embayments in the caldera rim which is very nearly circular (Table 1). The most prominent feature is an intra-caldera bench that extends around the two southern quadrants of the caldera with an elevation of about 40 m above the caldera floor. The bench is embayed to the south and west on its inward-facing edge but the continuity of the escarpment above the caldera floor suggests it was isolated by laterally extensive subsidence of the inner caldera floor. Detailed NASA TOPSAR topographic data indicate that the center of the bench is higher than both the inner and outer edges (Rowland and Mouginiis-Mark, 1993). This probably indicates that this central region has been built up by the eruption of material from arcuate fissures within the bench. An isolated cinder cone located adjacent to the caldera wall on the southwestern portion of the bench and a small circular pit to the south are further indicators that the magmatic plumbing extends through the bench (Rowland and Mouginiis-Mark, 1993). Talus slopes are present beneath the northern and eastern rims. A small terrace

Table 1
Comparison of caldera dimensions in the western Galápagos and Hawai'i

Volcáno Name	Maximum width (km)	Minimum width (km)	Maximum depth ^a (m)	Estimated volume ^a (km ³)	Area encompassed by caldera rim (km ²)	Ratio of subaerial area of shield to area encompassed by caldera rim
Volcán Wolf	6.4	5.1	660	9.3	22.8	23.2
Volcán Darwin	5.6	5.5	200	4.2	23.9	26.6
Volcán Alcedo	7.4	6.1	260	7.8	41.6	16.9
Sierra Negra	9.3	7.4	110	5.2	59.8	32.9
Cerro Azul	4.3	3.2	480	2.8	9.7	56.3
Volcán Fernandina	6.5	4.6	1100	12.4	20.1	27.1
Kilauea, Hawaii ^b	5.0	3.1	140	1.4	15.5	93.6
Mauna Loa, Hawaii ^b	4.5	2.7	176	1.0	11.7	438.0

^a Depth measurements are from the highest point of the caldera rim to the lowest elevation of the caldera floor. Taken from Defence Mapping Agency topographic maps where available and from Nordlie (1973).

^b Data from Walker (1988). The volume of Kilauea caldera was nearly 1 km³ greater in 1825. Variation in the volume of the central pit crater of Halemaumau has totalled 1.65 km³ since 1823 (Walker, 1988).

is situated beneath the northeastern segment of the caldera rim and is bounded on its inward side by a talus slope. To the north of this terrace, talus slopes extend from the caldera rim to the floor.

Flows originating from arcuate vents have reached the caldera floor from the eastern rim. A lava flow that issued from a vent on the caldera floor is visible in the SPOT image on the northeastern part of the

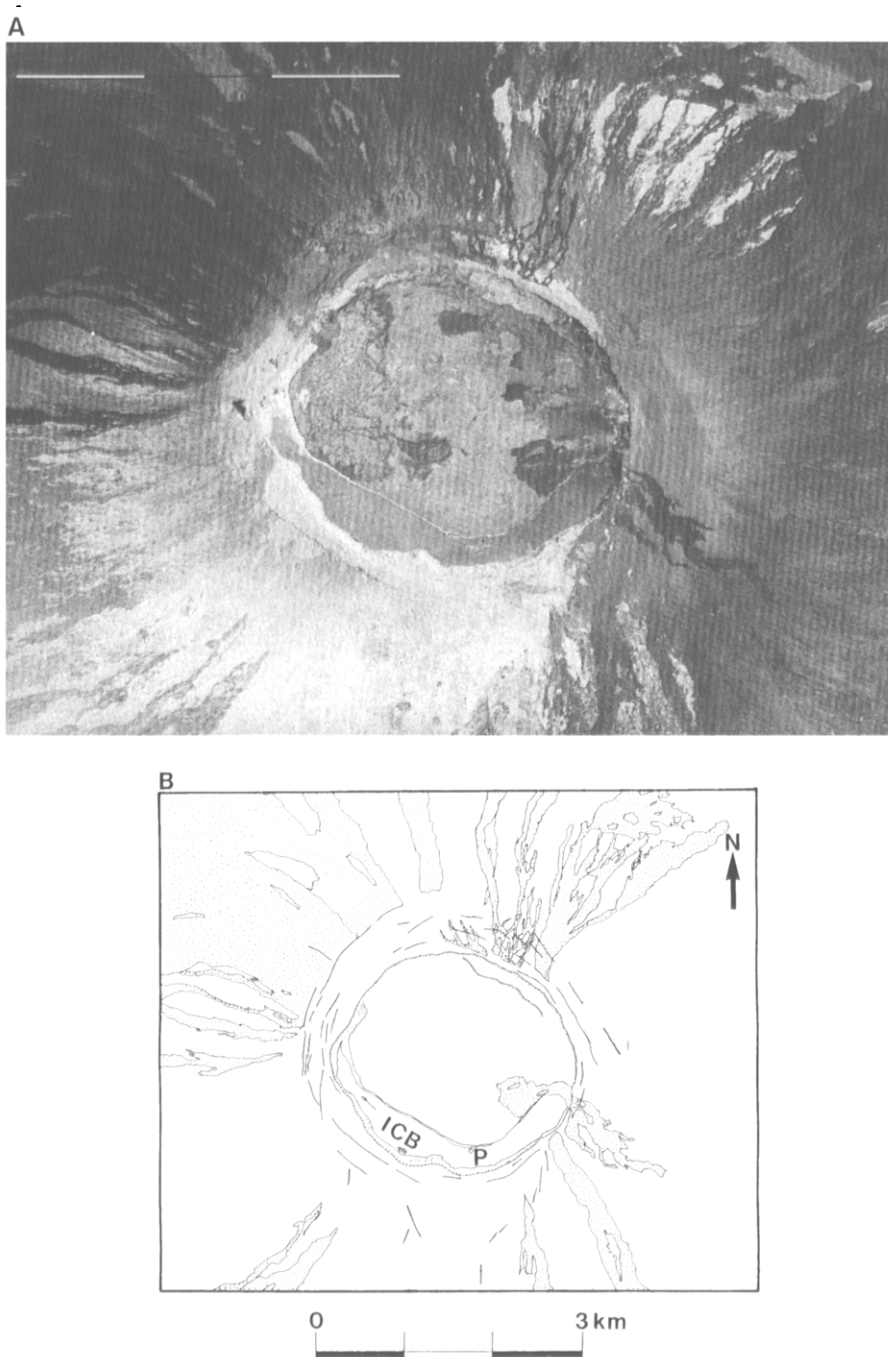


Fig. 3. The caldera of Volcán Darwin. (A) SPOT image. (B) Sketch map. *P* = pit. Key as for Fig. 2.

caldera floor. The web-like pattern is interpreted to be the disrupted surface of a ponded lava flow, and the TOPSAR data indicate that the crust of the flow had cooled to a thickness of about 10 m prior to remobilizing.

3.3. Volcán Alcedo

Volcán Alcedo is unusual amongst the major shield volcanoes of the western Galápagos in that its surface is blanketed with a rhyolitic pumice fall

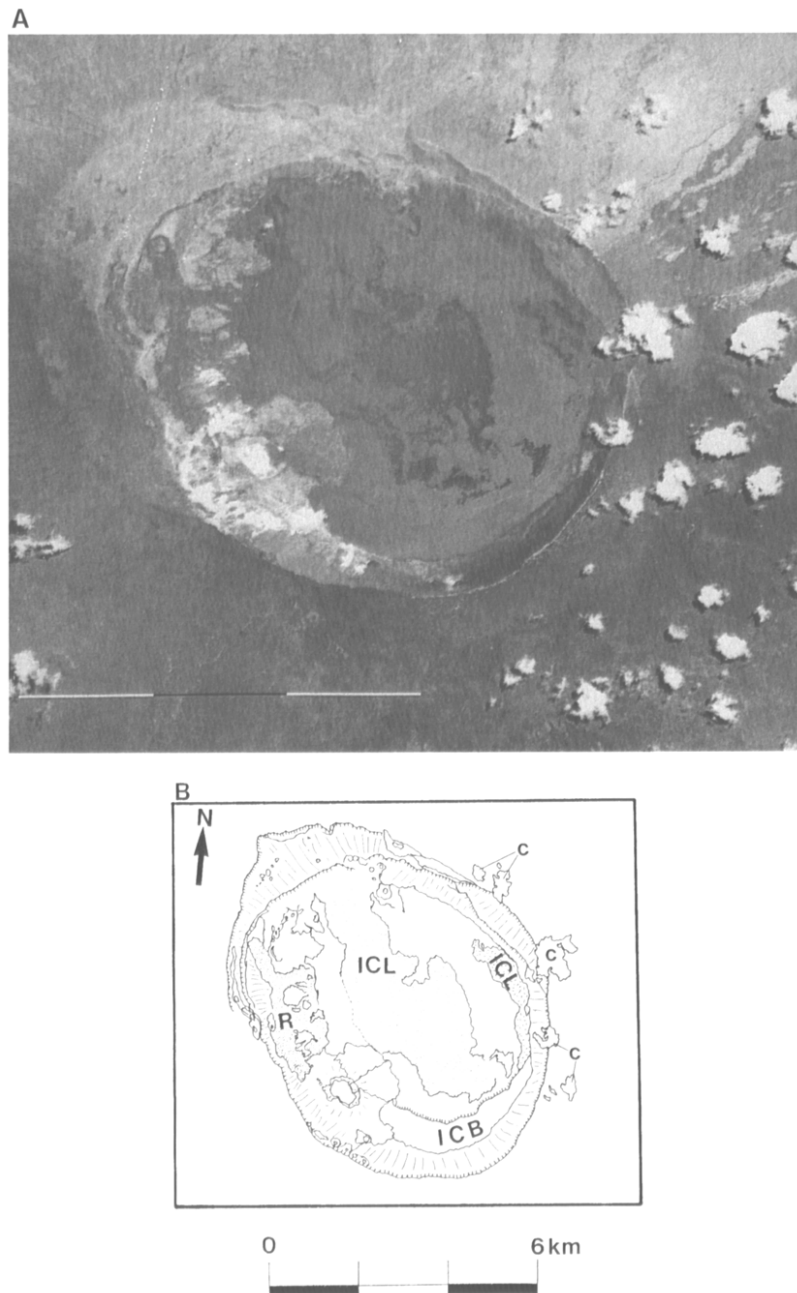


Fig. 4. The caldera of Volcán Alcedo. (A) SPOT HRV-1 image. (B) Sketch map. *R* = Rhyolite; *ICL* = Co-mingled intra-caldera lava. Key as for Fig. 2.

deposit (Geist et al., 1994) and a suite of silicic lavas has erupted within the caldera as well as on the southwestern flank (McBirney et al., 1985). The

caldera is slightly elongated along a NW–SE trend (Fig. 4), reaches a maximum depth of 240 m (Table 1) and lacks evidence of embayment of the caldera

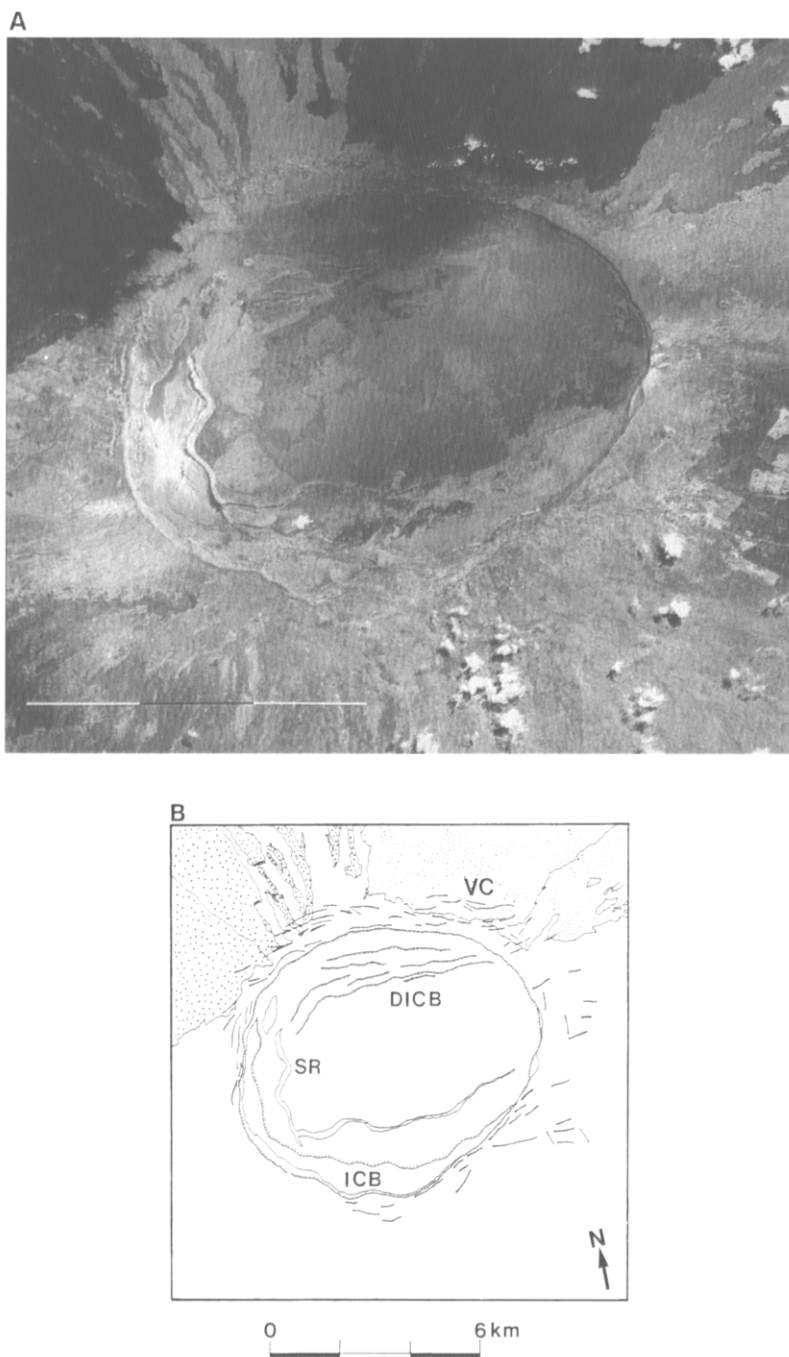


Fig. 5. The caldera of Sierra Negra. (A) SPOT HRV-1 image. (B) Sketch map. *SR* = sinuous ridge; *DICB* = discontinuous intra-caldera bench; *VC* = Volcán Chico area. Key as for Fig. 2.

rim by recent collapse. An intra-caldera bench exists at a height of ~ 100 m beneath the western and southern rim. Less continuous benches occur to the northeast.

3.4. *Volcán Sierra Negra*

With the largest caldera by area in the western Galápagos (59.8 km^2), Sierra Negra has a maximum

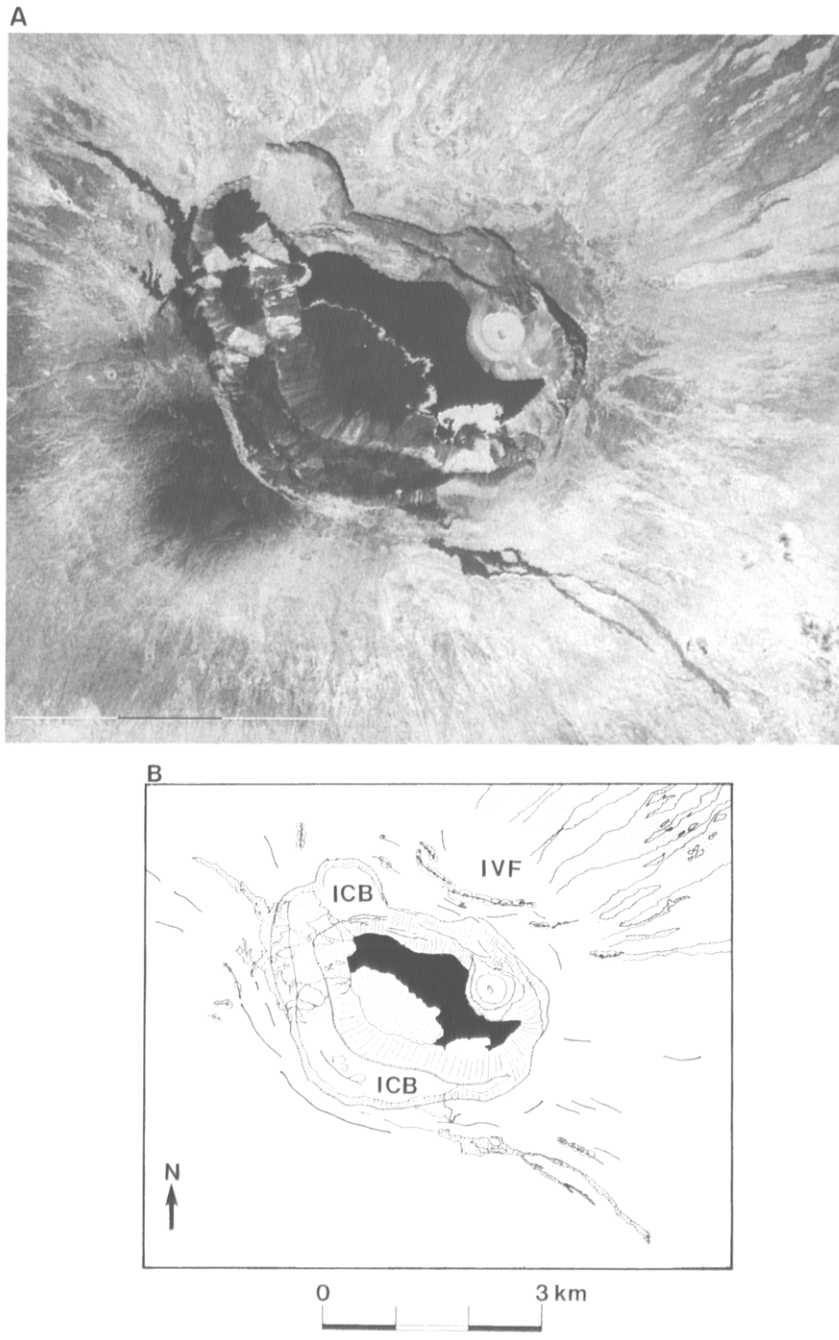


Fig. 6. The caldera of Cerro Azul. (A) SPOT HRV-1 image. (B) Sketch map. Heavy stipple = phreatomagmatic cone. Key as for Fig. 2.

depth of only 110 m. The caldera is slightly elongated along a WSW–ENE trend (Fig. 5) which has previously been interpreted as the result of the inter-

section of regional structural trends (Darwin, 1844; Nordlie, 1973). The floor of the caldera is the site of a sinuous ridge that is most distinctive around the

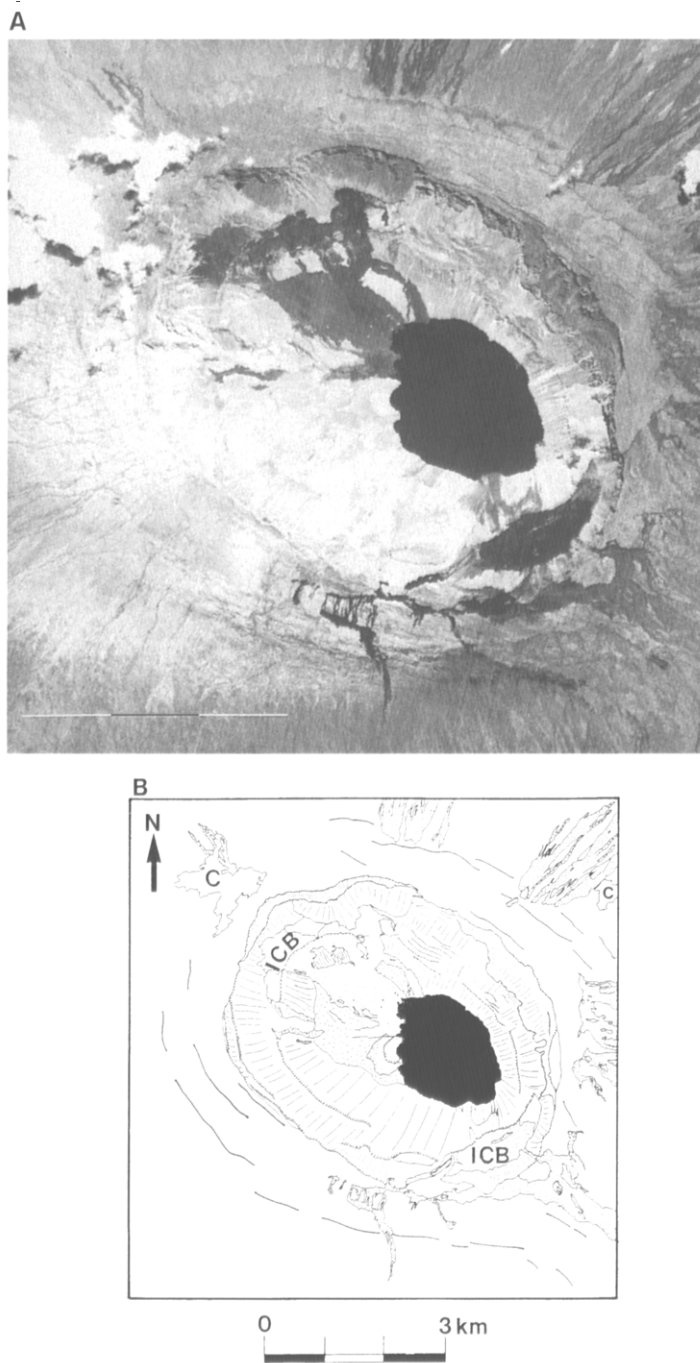


Fig. 7. The caldera of Volcán Fernandina. (A) SPOT HRV-1 image. (B) Sketch map. C = clouds in SPOT-1 image. Key as for Fig. 2.

western and southwestern perimeter and continues in a more subdued form toward the east. Field work by Reynolds and Geist (1991) indicated that the ridge was formed by numerous uplifted and down-dropped blocks, many of which have been tilted toward the center of the caldera. Based on the TOPSAR data, the crest of the ridge averages 60–100 m above the adjacent caldera floor. The bright area east of the ridge is the site of intense fumarolic activity that has produced alteration deposits, predominantly sulfates and opal (Delaney et al., 1973). The pattern of intra-caldera bench development at Sierra Negra shows a marked contrast between the northern and southern portions of the caldera. To the north, irregular movement of the caldera floor has produced a series of discontinuous benches that form terraces beneath the northern rim. To the south an extensive crescentic bench 40 m below the rim extends around the same portion of the caldera as the previously described sinuous ridge. Historic eruptive activity on Sierra Negra has originated within the Volcán Chico area adjacent to the northern rim (Delaney et al., 1973).

3.5. *Volcán Cerro Azul*

In area, the caldera of Cerro Azul is the smallest in the western Galápagos (Table 1), yet it shows the most complex development of rim embayments and intra-caldera benches (Fig. 6). The caldera is elongate along an ESE–WNW trend (Table 1). At its northwestern end the rim is scalloped by two embayments. The benches within these embayments are estimated from photographs to be at the same elevation 200 m beneath the rim and 450 m above the caldera floor (topographic data for Cerro Azul are not available from the DMA maps, and the TOPSAR data are corrupted at this particular location). It is thus probable that the collapse pits were once linked and flooded by the same lava flows. They were later incorporated into the main caldera. A third, less-prominent embayment occurs in the northern rim of the caldera. A major intra-caldera bench lies adjacent to the southern rim of the caldera. An arcuate vent system located close to the back of the southern bench has fed an extensive series of flows that cascaded to the caldera floor. A prominent cone is seen on the eastern segment of the caldera floor. The

morphology of this cone (see Steadman and Zoumer, 1988, p. 37) suggests that it was formed by phreatomagmatic activity indicating that an intra-caldera lake existed at the time of eruption. A small lake was visible during the May 1993 TOPSAR flight.

3.6. *Volcán Fernandina*

With a maximum depth of 1100 m, Fernandina has the deepest and most markedly elongated Galápagos calderas (Table 1). Embayments in the northwestern and southeastern sectors of the caldera rim extend the elliptical outline of the caldera (Fig. 7). Prominent benches occur within both embayments, the southeastern bench lies 300 m beneath the rim and the northwestern bench is 250 m beneath the rim. The flat-lying nature of the flows that comprise the southwestern bench indicates that they ponded within a closed depression which was united with the larger caldera by subsequent collapse (Rowland and Munro, 1992). The northern wall of the caldera shows many slumped blocks and a prominent break in slope at the level of the intra-caldera benches. The southwestern wall is marked by extensive talus slopes that descend from the caldera rim to the floor.

4. The significance of caldera size

Previous investigators have commented on the large size of the calderas of the western Galápagos volcanoes (e.g., Simkin and Howard, 1970; Nordlie, 1973). This point is illustrated in Table 1 which shows that their volumes are two–nine times that of Kilauea caldera and three–twelve times that of Mauna Loa, usually considered to be the type examples of basaltic shield volcanoes. The distribution of eruptions on the Galápagos shields, as indicated by eruptive fissures mapped from aerial photographs (Chadwick and Howard, 1991), provides an important clue to explain the large size of their calderas. In particular, Chadwick and Howard (1991) confirmed earlier observations (Simkin, 1972, 1984; Nordlie, 1973) that well-developed radial rift zones do not occur on these volcanoes. Subtle preferred trends for the alignment of fissures on the flanks of the volcanoes are present, but the spacing and co-linearity of

individual vents are not confined to distinctive narrow zones such as on Hawaiian shields (Chadwick and Howard, 1991; Munro, 1992). Additionally unlike Hawaiian shields, there is no evidence for the development of fault-bounded subsidence (graben) aligned with the subtle concentrations of radial fissures. In Hawai'i, these graben have been linked to prolonged magma storage within the rift zone (Delaney et al., 1990). Finally, the paucity of tube-fed pahoehoe lavas on the flanks of the Galápagos volcanoes (Williams and McBirney, 1979; Simkin, 1984) suggests that long-lasting low-effusion-rate eruptions are rare, in turn suggesting that efficient, unobstructed links between a shallow magma chamber and the surface (Rowland and Walker, 1990) are rarely established. This is in contrast to the Kilauea and Mauna Loa examples where tube-fed pahoehoe comprises 58 and 30%, respectively, of the present surface (Greeley, 1987). This evidence leads us to conclude that in the western Galápagos, magma storage is mostly restricted to a magma chamber beneath the central portion of each volcano, and the large caldera size is a reflection of this focus of magma storage.

5. The influence of calderas on eruptive fissure morphology

The summit regions of the western Galápagos volcanoes are noted for distinctive arcuate fissures that form in a circumferential pattern around the caldera rim (McBirney and Williams, 1969; Simkin, 1972; Simkin and Fiske, 1986; Chadwick and Howard, 1991). Although similar fissures have been observed in limited numbers at other volcanoes [e.g., Niuafu'ou, Tonga (Newhall and Dzurisin, 1988), Piton de la Fournaise on Reunion, and Deception Island (Baker et al., 1975)], their dominance in the summit regions of the western Galápagos seems to be unique amongst basaltic shield volcanoes. We propose that in the Galápagos, this pattern has developed as a consequence of a radially oriented least-compressive stress (σ^3) that is set up in the summit regions due to the large calderas.

The arcuate traces of the fissures may be explained by the structural effect of the caldera wall on subsurface dike propagation. A propagating dike is

attempting to grow in three directions (horizontal propagation, vertical propagation and horizontal widening). The most difficult of these is the widening meaning that the dike will preferentially orient itself so that this widening can work against σ^3 (e.g., Nakamura, 1977). Observations at Mt. Etna in the vicinity of the Vale del Bove, a major escarpment on the eastern flank, provide an essential analogy to the Galápagos case being examined here. Measurement of surface ground displacement during intrusion emplacement indicates that the Valle del Bove alters the near-surface stress regime such that the direction of dike propagation and subsequent fissure development is parallel to the trend of the escarpment (McGuire and Pullen, 1989; McGuire et al., 1990). The up to 1000-m-high Valle del Bove escarpment provides an unbuttressed surface orienting σ^3 perpendicular to its face. Dikes orient themselves so that their direction of widening is parallel to this σ^3 meaning that they are propagating parallel to the escarpment. Even if a dike initially propagates in a direction that would ultimately intersect the wall of the Valle del Bove, it deviates such that it becomes parallel (McGuire and Pullen, 1989).

The deep Galápagos calderas are analogous to the Valle del Bove except that rather than being the heads of large amphitheatres, they are closed depressions. Any dike approaching the summit in the vicinity of the calderas will be perturbed by this inwardly radial σ^3 and orient itself parallel to the caldera wall. Repeated collapses of the caldera walls provide a means for maintaining the stress regime that allows continued development of arcuate fissures. Such collapse is evident from the description of eruptions at Volcán Fernandina in 1988 (Chadwick et al., 1991) and 1991 (Perez-Oviedo, 1991). The calderas not only modify the orientations of dikes so that they form arcuate vents, but also provide the means for sustaining the conditions that lead to continued intrusive activity within the central zone of the volcano.

However, it is important to note that three of the six active calderas (Darwin, Alcedo and Sierra Negra) are not particularly deep, yet arcuate fissures still occur in profusion around them. For example, most historic Sierra Negra eruptions have occurred from an arcuate fissure complex (Volcán Chico; Delaney et al., 1973), so it is clear that arcuate dikes will develop in the vicinity of shallow Galápagos

calderas as well. These shallow calderas are infilled with ponded lavas which are probably sagging into the center of the volcano (e.g., Walker, 1988). This inward sagging may be sufficient to maintain a radial σ^3 in the summit region even when the calderas are nearly infilled. Thus the pattern of arcuate fissure development may be sustained throughout volcano construction.

6. Mechanisms for caldera formation on the Galápagos islands

The western Galápagos calderas can be grouped into two categories based on their present depths. There is no way of surmising whether or not the patterns we observe today prevailed throughout the construction of the edifice, although this seems unlikely; studies in Hawai'i have shown that basaltic calderas infill and collapse many times during the life of the volcano (Holcomb, 1987; Lockwood and Lipman, 1987; Decker, 1987). The calderas of Wolf, Cerro Azul and Fernandina are characterized by larger depth-to-diameter ratios as well as evidence for localized subsidence within the caldera, producing a funnel-like morphology. Their morphology suggests that recent rates of subsidence have far outstripped recent rates of infilling. These three calderas also show development of benches within major embayments of the caldera rim.

With present data it is difficult to assess the relationship between the height of these caldera escarpments (up to ~ 900 m) and the rate at which subsidence occurs. Rapid subsidence by 350 m of the southeastern portion of the caldera floor at Fernandina was recorded by Simkin and Howard (1970) but it did not produce a major escarpment, despite causing major displacement of intra-caldera talus. The development of huge talus fans banked against the intra-caldera scarps, many of which are vegetated, suggests that such large subsidence events are infrequent. Additionally, many of the talus fans extend from the caldera floor almost to the bench tops or even the caldera walls suggesting that accumulation has continued for extensive periods of time. This suggests that subsidence may result from a series of small events insufficient to displace the talus fans but in total sufficient to produce major escarpments.

The calderas of Darwin, Alcedo and Sierra Negra show low depth-to-diameter ratios and limited evidence for recent subsidence events. The caldera rims show no embayments and intra-caldera benches are not prominent.

Two scenarios that may be responsible for the variation in caldera size and the patterns of subsidence in the Galápagos are: (1) that caldera subsidence is a function of the relationship between the rate at which lavas infill the caldera and the rate at which magma is withdrawn from the magma chamber; (2) or that the shape of the magma storage complex determines the dimensions and subsidence behavior of each caldera. Studies of Mauna Loa and Kilauea (King, 1989) show that magma supply rates to these volcanoes from their common mantle source are approximately the same over periods of 10^4 years but over shorter time spans ($< 10^2$ years) either volcano may dominate the eruptive record (and by inference magma supply; Klein, 1982). In the western Galápagos, nine volcanoes may be "competing" for the same mantle magma source (historic eruptions have also been recorded on Santiago, Marchena and Pinta islands; Simkin and Seibert, 1994). Thus for our first scenario, it is possible that structural conditions at individual volcanoes may provide a (perhaps temporally varying) preferential environment for the transport of magma. The deeper calderas (Wolf, Cerro Azul and Fernandina) may be currently in a phase of high magma supply rate whereas those that are shallower (Darwin, Alcedo and Sierra Negra) may be currently supplied at lower rates. The former group would be expected to erupt more frequently (which is the case for the historical record) because the higher supply rates lead to more rapid overpressuring of the magma-chamber walls. As long as replenishment of the magma chamber proceeds at a slower rate than the time-averaged discharge during eruptions, these eruptions would eventually lead to an unsupported roof and, in turn, to collapse.

There is little evidence to support a direct relationship between eruptions and collapse. In 1968, the collapse of the caldera floor at Volcán Fernandina resulted in an increase in caldera volume of $1\text{--}2\text{ km}^3$ but the total volume of magma (estimated from the extent of lava flows and tephra deposits) that was erupted subaerially was less than 0.1 km^3 , and no

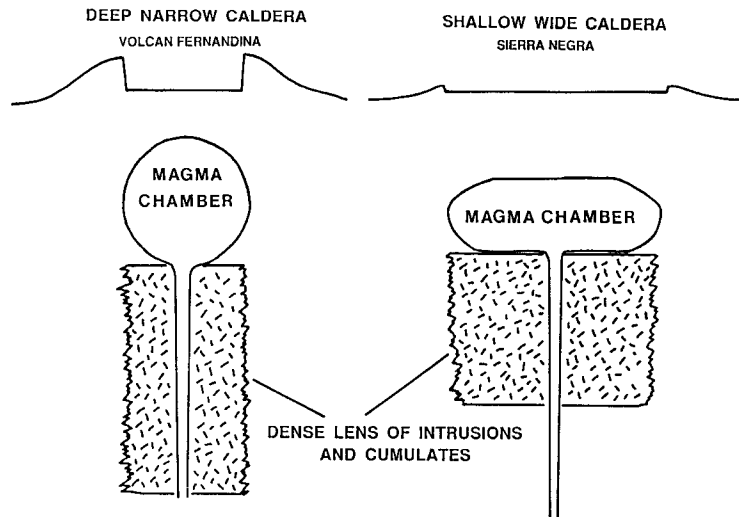


Fig. 8. The proposed effect of variation in the shape of a coherent intrusive sheet complex (Walker, 1988, 1992) on caldera morphology.

evidence was seen for the occurrence of large submarine eruptions that might compensate for the discrepancy in volumes (Simkin and Howard, 1970). More likely the small erupted volume was sufficient to trigger what had been a potential collapse that had been built up by numerous previous eruptions. Additionally, the 1979 eruption Sierra Negra produced 0.3–0.6 km³ of lava with no recorded collapse. This volume is based on a lava delta that covers a surface area of 56 km² (mapped in SPOT data; Munro, 1992), with an estimated thickness of 5–10 m.

The second scenario to explain the variations in size and morphology of the Galápagos calderas is that they are dependent on the morphology of a coherent intrusive sheet complex (Walker, 1988, 1992). As the volcano grows, an intrusive sheet complex develops at the base of the central magma chamber, in part because of limited lateral movement of the volcano flanks. Fig. 8 is an idealized representation of the manner in which the variation in morphology of an intrusive sheet complex may influence the size and morphology of a basaltic caldera. Where the development of the sheet complex is laterally restricted, the same volume of subsidence produces a deeper caldera (i.e., Wolf, Cerro Azul, Fernandina) and vice versa (i.e., Darwin, Alcedo, Sierra Negra). Significantly, this alternative model implies that the morphological characteristics of each caldera will be relatively constant for long periods of time, perhaps

throughout the life of the volcano. This is unlike the varying-supply model where we might expect to see a wide variety of subsidence behavior over long periods of time and consequently a greater range of caldera morphologies at each shield.

The existence of an intrusive sheet complex beneath the calderas of the Galápagos shield volcanoes can currently only be considered as conjecture. Such structures have been proposed to have existed beneath major Tertiary volcanic centers in Scotland (Walker, 1992) but may only be observed at considerable erosional depths. However, as pointed out above, it is equally difficult to present convincing evidence for a model of caldera formation related to magma supply rates.

7. Conclusions

The distribution and characteristics of eruptive activity and the morphology of the calderas of the major shield volcanoes of the western Galápagos, as interpreted from SPOT-1 satellite images, suggest that the calderas evolve in association with a central magma chamber that is essentially the sole site of magma storage for each volcano. The caldera walls impose a structural regime that favors the development of arcuate fissures adjacent to the caldera rim. The calderas show a variation in patterns of subsi-

dence that suggest the nature of magma storage within the edifice is unique for each shield. Two possible mechanisms are considered for the development of the Galápagos calderas: (1) repeated evacuation and replenishment of a high-level magma chamber at differing rates for each volcano; (2) development of coherent intrusive complexes with varying morphologies. There is no doubt that more data are needed to constrain these scenarios, and of particular importance is a better understanding of the ratios of intrusive to extrusive volcanics within Galápagos volcanoes. Possibly characterization of the internal density structure of these volcanoes using seismic or gravity data would yield significant insight to this problem.

Acknowledgements

This paper is dedicated to Victor-Hugo Perez-Oviedo who accompanied the authors to Volcán Fernandina in 1989 and who died in the March 1993 eruption of Guagua Pichincha, Ecuador. The assistance of the personnel of the Charles Darwin Research Station, Peter Mouginiis-Mark and Lionel Wilson during the same expedition is gratefully acknowledged. The authors wish to thank William Chadwick, Robert Tilling and Greg Valentine for their thorough reviews of the manuscript. This work was supported by grant NAGW-1162 from the NASA Geology program and JPL SIR-C Program Contract #958457 (PI for both: Peter Mouginiis-Mark). This is HIGP publication number 886 and SOEST contribution number 4084.

References

- Baker, P.E., McReath, I., Harvey, M.R., Roobol, M.J. and Davies, T.G., 1975. The geology of the South Shetland Islands, V, volcanic evolution of Deception Island. *Br. Antarct. Surv. Sci. Rep.* 78, 81 pp.
- Chadwick, W.W. and Howard, K.A., 1991. The pattern of circumferential and radial eruptive fissures on the volcanoes of Fernandina and Isabela islands, Galápagos. *Bull. Volcanol.*, 53: 259–275.
- Chadwick, W.W., DeRoy, T. and Carrasco, A., 1991. The September 1988 intracaldera avalanche and eruption at Fernandina volcano, Galápagos Islands. *Bull. Volcanol.*, 53: 276–286.
- Chevrel, M., Courtois, M. and Weill, G., 1981. The SPOT satellite remote sensing mission. *Photogramm. Eng. Remote Sens.*, 47: 1163–1171.
- Darwin, C.R., 1844. *Geological Observations on Volcanic Islands*. Smith, Elder and Co, London.
- Decker, R.W., 1987. Dynamics of Hawaiian volcanoes: an overview. *U.S. Geol. Surv., Prof. Pap.*, 1350: 997–1018.
- Delaney, J.R., Colony, W.E., Gerlach, T.M. and Nordlie, B.E., 1973. Geology of the Volcan Chico area on Sierra Negra volcano, Galápagos Islands. *Geol. Soc. Am. Bull.*, 84: 2455–2470.
- Delaney, P.T., Fiske, R.S., Miklius, A., Okamura, A.T. and Sako, M.K., 1990. Deep magma body beneath the summit and rift zones of Kilauea volcano, Hawaii. *Science*, 247: 1311–1316.
- Dutton, C.E., 1884. Hawaiian volcanoes. *U.S. Geol. Surv., Annu. Rep.*, 4: 75–219.
- Evans, D.L., Farr, T.G., Zebker, H.A., Van Zyl, J.J. and Mouginiis-Mark, P.J., 1992. Radar interferometric studies of the Earth's topography. *EOS*, 73: 553–558.
- Farr, T., Evans, D., Zebker, H., Harding, D., Bufton, J., Dixon, T., Vetrilla, S. and Gesch, D., 1995. Mission in the works promises precise global topographic data. *EOS*, 76: 225–229.
- Geist, D.J., Howard, K.A., Jellinek, A.M. and Rayder, S., 1994. Volcanic history of Volcán Alcedo, Galápagos Archipelago: A case study of rhyolitic oceanic volcanism. *Bull. Volcanol.*, 56: 243–260.
- Greeley, R., 1987. The role of lava tubes in Hawaiian volcanoes. *U.S. Geol. Surv., Prof. Pap.*, 1350: 1580–1602.
- Holcomb, R.T., 1987. Eruptive history and long-term behavior of Kilauea Volcano. *U.S. Geol. Surv., Prof. Pap.*, 1350: 261–350.
- King, C.Y., 1989. Volume predictability of historical eruptions at Kilauea and Mauna Loa volcanoes. *J. Volcanol. Geotherm. Res.*, 38: 281–285.
- Klein, F.W., 1982. Patterns of historical eruptions at Hawaiian volcanoes. *J. Volcanol. Geotherm. Res.*, 12: 1–16.
- Lockwood, J.P. and Lipman, P.W., 1987. Holocene eruptive history of Mauna Loa Volcano. *U.S. Geol. Surv., Prof. Pap.*, 1350: 509–535.
- Macdonald, G.A., 1965. Hawaiian calderas. *Pac. Sci.*, 19: 320–334.
- McBirney, A.R. and Williams, H., 1969. Geology and petrology of the Galápagos Islands. *Geol. Soc. Am. Mem.* 118, 197 pp.
- McBirney, A.R., Cullen, A.B., Geist, D., Duncan, R.A., Hall, M.J. and Estrella, M., 1985. The Galápagos volcano Alcedo: A unique ocean caldera. *J. Volcanol. Geotherm. Res.*, 26: 173–177.
- McGuire, W.J. and Pullen, A.D., 1989. Location and orientation of eruptive fissures and feeder-dykes at Mount Etna: influence of gravitational and regional tectonic stress regimes. *J. Volcanol. Geotherm. Res.*, 38: 325–344.
- McGuire, W.J., Pullen, A.D. and Saunders, S.J., 1990. Recent dyke-induced large-scale block movement at Mount Etna and potential slope failure. *Nature*, 343: 357–359.
- McLelland, L., Simkin, T., Summers, M., Nielsen, E. and Stein, T.C., 1989. *Global Volcanism 1975–1985. The First Decade of Reports from the Smithsonian Institutions' Scientific Event Alert Network (SEAN)*. Prentice Hall, Englewood Cliffs, NJ, 657 pp.

- Munro, D.C., 1992. The application of remotely sensed data to studies of volcanism in the Galápagos Islands. Ph.D. Thesis, Univ. Hawai'i.
- Nakamura, K., 1977. Volcanoes as possible indicators of tectonic stress orientation – principle and proposal. *J. Volcanol. Geotherm. Res.*, 2: 1–16.
- Newhall, C.G. and Dzurisin, D., 1988. Historical unrest at large calderas of the world. *U.S. Geol. Surv. Bull.* 1855, 1108 pp.
- Nordlie, B.E., 1973. Morphology and structure of the western Galápagos volcanoes and a model for their origin. *Geol. Soc. Am. Bull.*, 84: 2931–2956.
- Perez-Oviedo, V., 1991. Teledetección de la erupción del 19 abril de 1991 en la Isla Fernandina. *Inf. Intern. CLIRSEN*.
- Reynolds, R. and Geist, D.J., 1991. Structure and eruptive style of Sierra Negra volcano, Isla Isabela, Galápagos Archipelago. *EOS*, 72: 313.
- Rowland, S.K. and Mouginiis-Mark, P.J., 1993. The structure of basaltic shield volcanoes from TOPSAR airborne radar: Volcán Darwin and potentially Mauna Loa. *EOS*, 74(43, suppl.): 641–642.
- Rowland, S.K. and Munro, D.C., 1992. The caldera of Volcan Fernandina: a remote sensing study of its structure and activity. *Bull. Volcanol.*, 55: 97–109.
- Rowland, S.K. and Walker, G.P.L., 1990. Pahoehoe and aa in Hawaii: volumetric flow rate controls the lava structure. *Bull. Volcanol.*, 52: 615–628.
- Simkin, T., 1972. Origin of some flat topped volcanoes and guyots. *Geol. Soc. Am. Mem.*, 132: 183–193.
- Simkin, T., 1984. Geology of the Galápagos Islands. In: R. Perry (Editor), *Galápagos*. Pergamon Press, Oxford, pp. 15–41.
- Simkin, T. and Fiske, R.S., 1986. Volcano growth dominated by circumferential feeding systems: A morphogenetic comparison of Galápagos volcanoes with young volcanic seamounts. *IAV-CEI Volcanol. Congr.*, Hamilton (not in abstract volume).
- Simkin, T. and Howard, K.A., 1970. Caldera collapse in the Galápagos Islands, 1968. *Science*, 169: 429–437.
- Simkin, T. and Seibert, L., 1994. *Volcanoes of the World*. Geoscience Press, Tuscon, AZ, 2nd ed., 349 pp.
- Steadman, D.W. and Zousmer, S., 1988. *Galápagos: Discovery on Darwin's Islands*. Smithsonian Inst. Press, Washington, DC, 208 pp.
- Walker, G.P.L., 1988. Three Hawaiian calderas: an origin through loading by shallow intrusions. *J. Geophys. Res.*, 93: 14,773–14,784.
- Walker, G.P.L., 1992. “Coherent intrusion complexes” in large basaltic volcanoes – a new structural model. *J. Volcanol. Geotherm. Res.*, 50: 41–54.
- Williams, H. and McBirney, A.R., 1979. *Volcanology*. Freeman Cooper, San Francisco, CA, 397 pp.
- Zebker, H.A., Madsen S.N., Martin, J., Alberti, G., Vetrilla, S. and Cucci, A., 1992. The TOPSAR interferometric radar topographic mapping instrument. 3rd Annu. J.P.L. Airborne Geosci. Workshop Summaries. Jet Propulsion Lab. Publ., 92-14(3): 49–52.